

**Functional Modulators and Missing-Linker Defects Realize High
Proton Conductivity in UiO-66-Hf Metal-Organic Frameworks**

*Fang Fang, Peng Wang, Zhen Zhang, Suo-Shu Zhang, Yuan-Yuan Guo,
Shu-Yu Wang, Lin Du * and Qi-Hua Zhao **

Key Laboratory of Medicinal Chemistry for Natural Resource, Ministry of Education and Yunnan Province, Yunnan Characteristic Plant Extraction Laboratory, School of Chemical Science and Technology, Yunnan University, 650500, People's Republic of China.

* Corresponding author.

E-mail: qhzhao@ynu.edu.cn; lindu@ynu.edu.cn

KEYWORDS: Metal-organic frameworks; Defect; Proton conductivity

Content

| | |
|---|-----------|
| 1. Synthesis Details..... | 1 |
| 1.1. Materials and Reagents..... | 1 |
| 1.2. Synthesis..... | 1 |
| 1.3. Activation..... | 1 |
| 1.4. Characterization..... | 1 |
| 2. Experimental Methods..... | 2 |
| 2.1. Thermal Gravimetric Analyzer (TGA)..... | 2 |
| 2.2. Nitrogen Sorption Measurements..... | 3 |
| 2.3. Scanning Electron Microscopy (SEM) and Energy-dispersive Spectrometry (EDS)..... | 4 |
| 2.4. Proton Conductivity..... | 5 |
| 2.5. Arrhenius plots..... | 7 |
| 2.6. Water vapor adsorption..... | 7 |
| 2.7. Power X-Ray Diffraction (PXRD) after textng proton conductivity..... | 8 |
| 3. Quantitative Analysis Methods..... | 9 |
| 3.1. Thermal Gravimetric Analyzer..... | 9 |
| 3.2. Proton Conductivity..... | 10 |
| 4. References..... | 10 |

1. Synthesis Details

1.1. Materials and Reagents

All chemicals and solvents are commercially sourced. All solvents are analytical grade reagents. All reagents used are analytically pure grade reagents purchased through formal commercial channels, and those not specifically indicated are used directly without purification. Ultrapure water ($18.2 \Omega \cdot \text{cm}^{-1}$) was prepared by Easy-15 ultrapure water system (Shanghai, China) and used to prepare all solutions and clean instruments during the experiment.

1.2. Synthesis

UiO-66 sample synthesis is a modification of the previously reported synthesis procedure [1] [2]. The synthesis process involves the formation of several defective UiO-66 frameworks by controlling the stoichiometry of terephthalic acid and monocarboxylic acid regulators. The doses for the several samples are listed in **Table S1**. Secondly, a mixture of hafnium chloride, terephthalic acid and monocarboxylic acid regulator and 20 ml DMF solvent were added to a 50 ml round bottom flask and synthesized by the one-pot method. Finally, the resulting slightly turbid colorless solution (note the smoke) is sonicated at room temperature until the smoke disappears and then stirred in oil bath with 80°C for 24 h. Elemental analyses (%) for UiO-66-NH₂-3.21 Found C:14.79, H:3.74, N:0.54; UiO-66-NH₂-3.02 Found C:15.04, H:4.11, N:0.00; UiO-66-NH₂-3.18 Found C:15.12, H:3.65, N:0.11; UiO-66-SO₃-2.36 Found C:17.57, H:2.47, S:2.55; UiO-66-SO₃-2.02 Found C:17.88, H:2.87, S:0.89; UiO-66-SO₃-3.30 Found C:15.63, H:3.56, S:0.09.

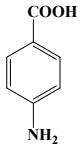
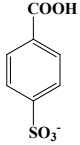
1.3. Activation

We put the resulting white powder in a beaker, add 20 ml of methanol, stir at room temperature for 4 h to filter. Then add 20 ml of methanol, repeat these steps above 3 times.

1.4. Characterization

Elemental analysis (C, H, N, S) were measured on the Flashsmart Analyser. Powder X-Ray diffraction (PXRD) measurements were done by the RIGAKUTTRIII-18kW (Cu-K α , $\lambda = 1.5418 \text{ \AA}$, 2θ scan in the range of $3\text{-}55^\circ$). Fourier Transform infrared spectra (FT-IR) were got on the Nicoletis10 Fourier Transform Infrared Spectroscope. SEM images were taken with a ZEISS Gemini 300 SEM operated at 3 kV. Thermogravimetric analysis (TG) dates were measured at STA449F3 (N₂ atmosphere, The temperature range is 25°C - 800°C and the heating rate is $10^\circ\text{C}\cdot\text{min}^{-1}$). Water vapor adsorption and Balanced-Emitter-Transister (BET) measurement were completed on American Quantachrome Autosorb-IQ.

Table S1. Molar ratios and the various reagents used in the UiO-66 syntheses.

| Modulator structure | HfCl ₄ (mmol) | BDC: Modulator (mmol) | | |
|---|--------------------------|-----------------------------------|-----------------------------------|-----------------------------------|
|  | 1.6 | 0.6:1.0 | 1.2:0.4 | 1.4:0.2 |
| | | UiO-66-NH₂-3.21 | UiO-66-NH₂-3.02 | UiO-66-NH₂-3.18 |
|  | 1.6 | 0.6:1.0 | 1.2:0.4 | 1.4:0.2 |
| | | UiO-66-SO₃-2.36 | UiO-66-SO₃-2.02 | UiO-66-SO₃-3.30 |

2. Experimental Methods

2.1. Thermal Gravimetric Analyzer (TGA)

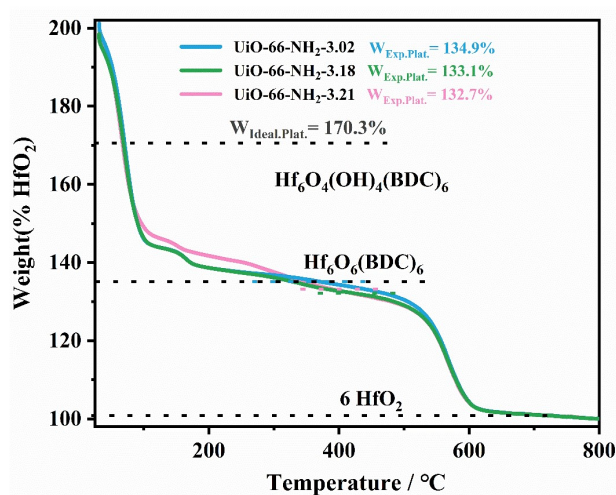


Figure S1. Thermogravimetric analysis (TGA) curves of UiO-66-NH₂-x (x = 3.02, 3.18, 3.21).

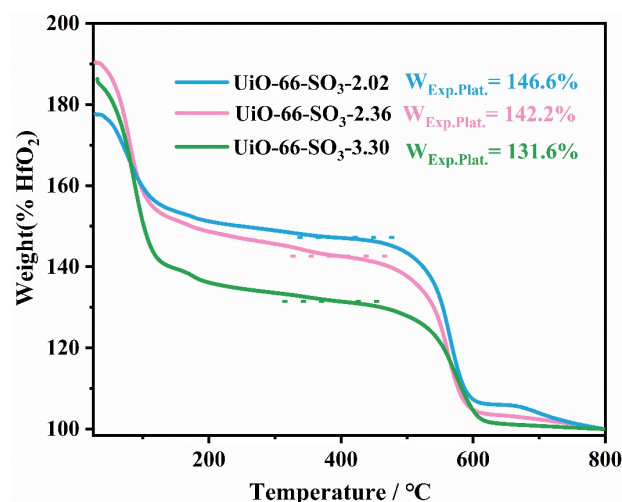


Figure S2. Thermogravimetric analysis (TGA) curves of UiO-66-SO₃-*x* (*x* = 2.02, 2.36, 3.30).

Table S2. The Temperature of Dehydroxylation (°C).

| | | | |
|------------------|------------------------------|------------------------------|------------------------------|
| Samples | UiO-66-NH ₂ -3.21 | UiO-66-NH ₂ -3.02 | UiO-66-NH ₂ -3.18 |
| Temperature (°C) | 132.7 | 134.9 | 133.1 |
| samples | UiO-66-SO ₃ -2.36 | UiO-66-SO ₃ -2.02 | UiO-66-SO ₃ -3.30 |
| Temperature (°C) | 142.7 | 146.6 | 131.6 |

2.2. Nitrogen Sorption Measurements

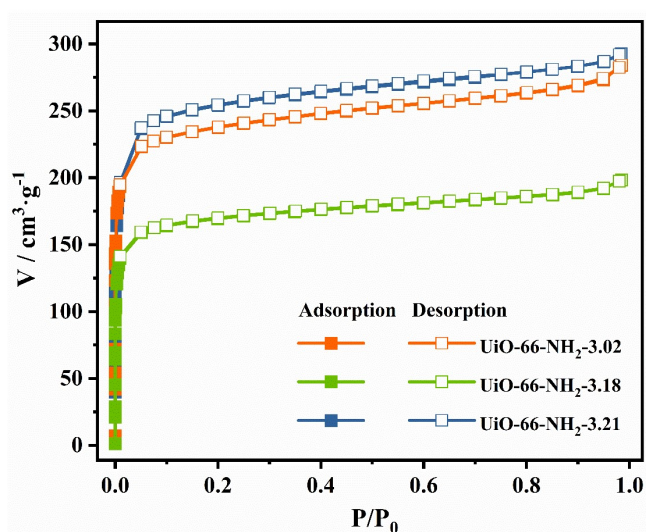


Figure S3. Nitrogen gas adsorption (closed circles) and desorption (open circles) isotherms of UiO-66-NH₂-*x* (*x* = 3.02, 3.18, 3.21) measured at 77 K.

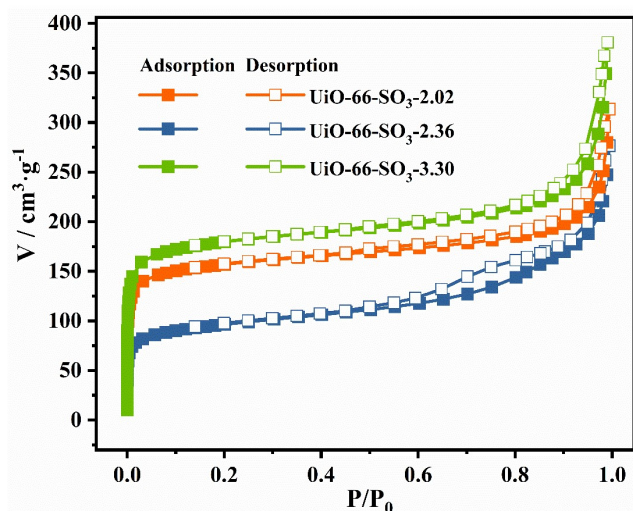


Figure S4. Nitrogen gas adsorption (closed circles) and desorption (open circles) isotherms of UiO-66-SO₃-x (x = 2.02, 2.36, 3.30) measured at 77K.

Table S3. The BET surface area (m²·g⁻¹).

| | | | |
|---|------------------------------|------------------------------|------------------------------|
| Samples | UiO-66-NH ₂ -3.21 | UiO-66-NH ₂ -3.02 | UiO-66-NH ₂ -3.18 |
| Surface Area (m ² ·g ⁻¹) | 997.2 | 932.3 | 664.9 |
| samples | UiO-66-SO ₃ -2.36 | UiO-66-SO ₃ -2.02 | UiO-66-SO ₃ -3.30 |
| Surface Area (m ² ·g ⁻¹) | 356.2 | 596.8 | 683.4 |

2.3. Scanning Electron Microscopy (SEM)

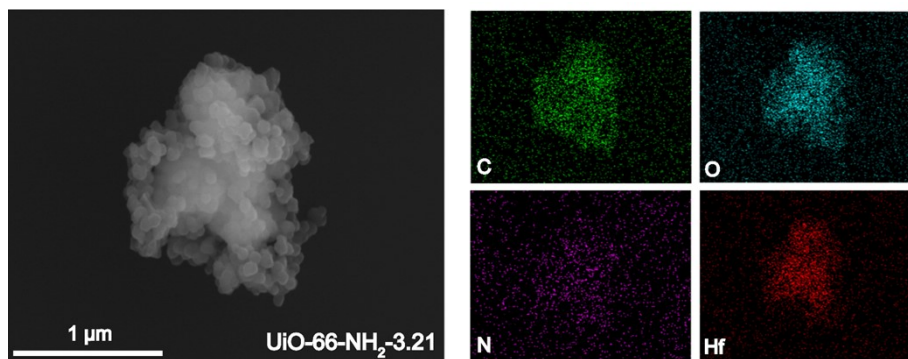


Figure S5. The EDS mapping images of UiO-66-NH₂-3.21.

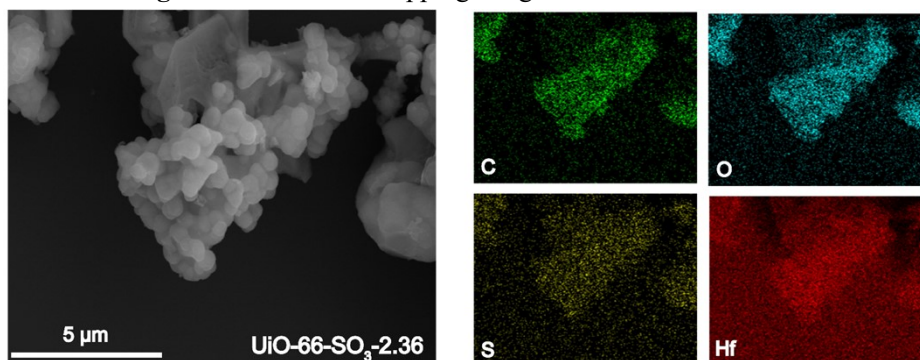


Figure S6. The EDS mapping images of UiO-66-SO₃-2.36.

2.5. Proton Conductivity

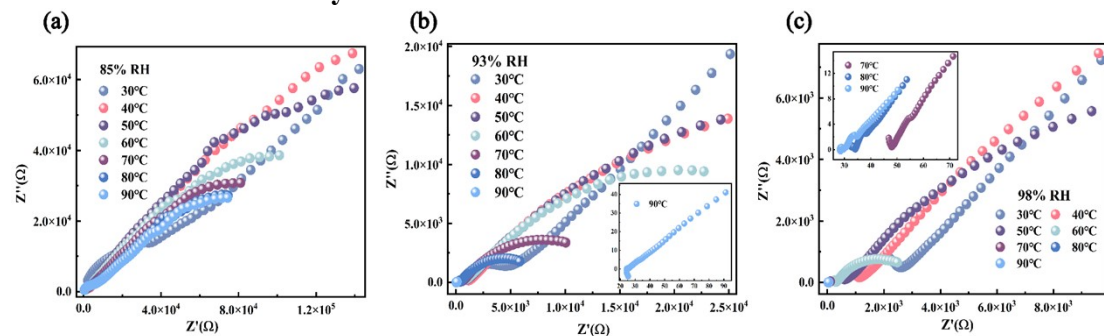


Figure S7. (a) Nyquist plot of **UiO-66-NH₂-3.02** measured at 30–90 °C, 85%RH, (b) Nyquist plot of **UiO-66-NH₂-3.02** measured at 30–90 °C, 93%RH, (c) Nyquist plot of **UiO-66-NH₂-3.02** measured at 30–90 °C, 98%RH.

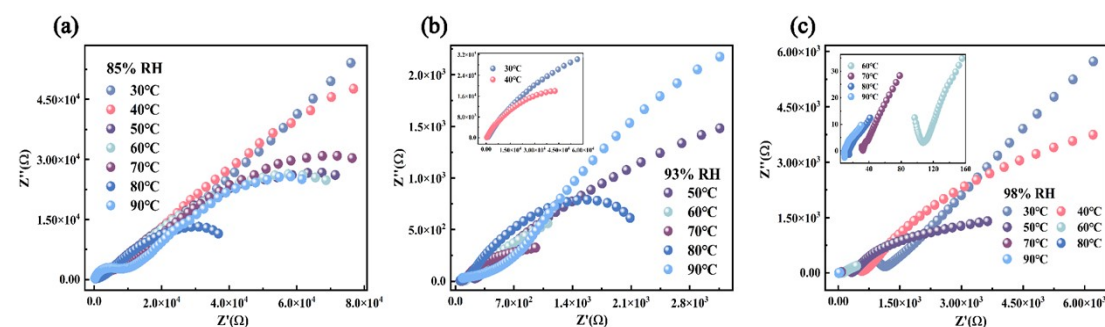


Figure S8. (a) Nyquist plot of **UiO-66-NH₂-3.18** measured at 30–90 °C, 85%RH, (b) Nyquist plot of **UiO-66-NH₂-3.18** measured at 30–90 °C, 93%RH, (c) Nyquist plot of **UiO-66-NH₂-3.18** measured at 30–90 °C, 98%RH.

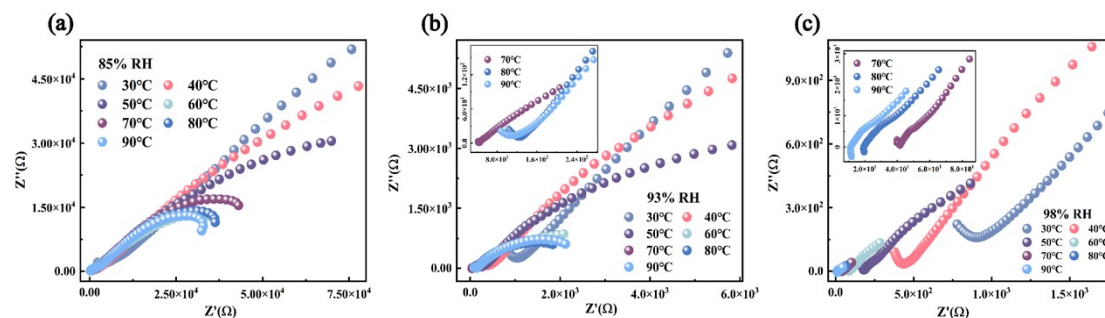


Figure S9. (a) Nyquist plot of **UiO-66-NH₂-3.21** measured at 30–90 °C, 85%RH, (b) Nyquist plot of **UiO-66-NH₂-3.21** measured at 30–90 °C, 93%RH, (c) Nyquist plot of **UiO-66-NH₂-3.21** measured at 30–90 °C, 98%RH.

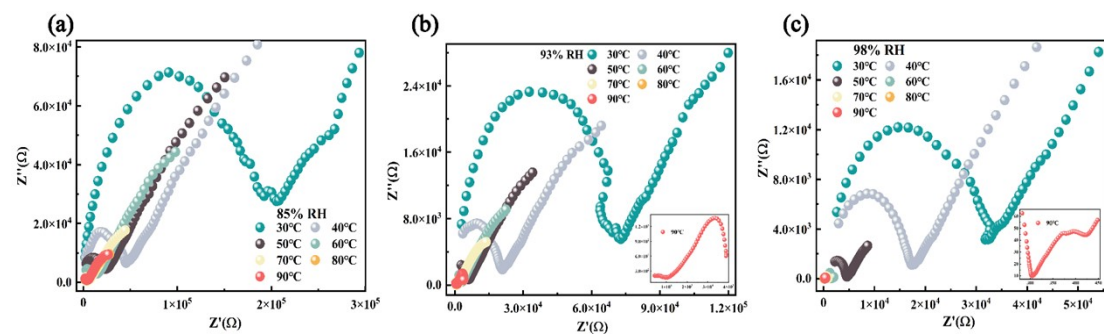


Figure S10. (a) Nyquist plot of **UiO-66-SO₃-2.02** measured at 30–90 °C, 85%RH, (b) Nyquist plot

of **UiO-66-SO₃-2.02** measured at 30–90 °C, 93%RH, (c) Nyquist plot of **UiO-66-SO₃-2.02** measured at 30–90 °C, 98%RH.

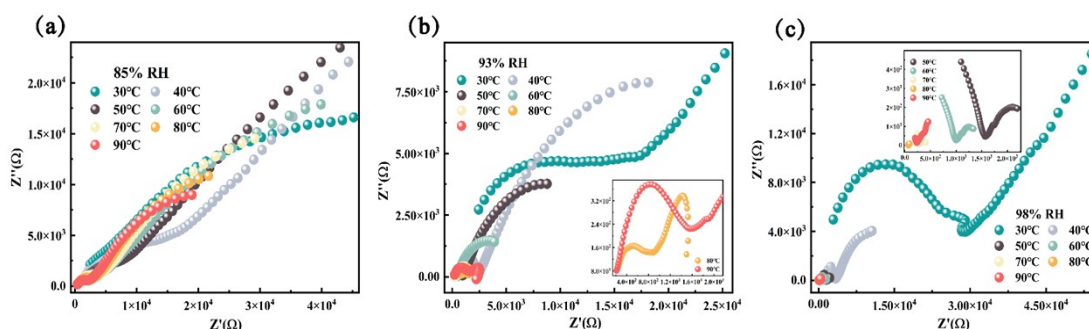


Figure S11. (a) Nyquist plot of **UiO-66-SO₃-2.36** measured at 30–90 °C, 85%RH, (b) Nyquist plot of **UiO-66-SO₃-2.36** measured at 30–90 °C, 93%RH, (c) Nyquist plot of **UiO-66-SO₃-2.36** measured at 30–90 °C, 98%RH.

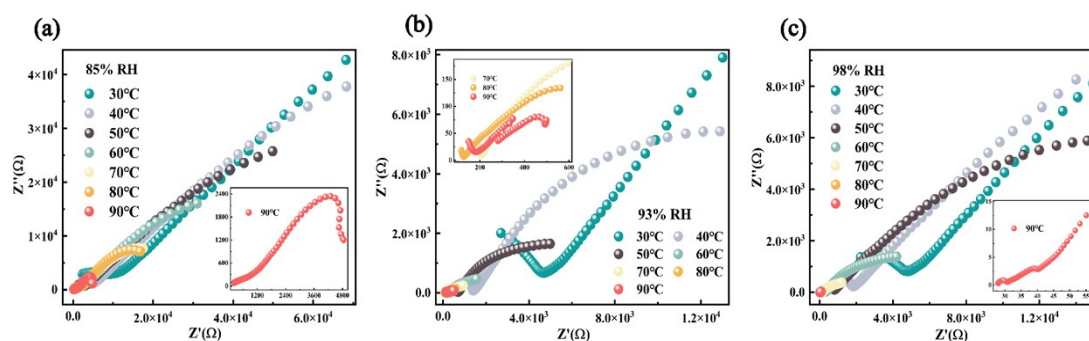


Figure S12. (a) Nyquist plot of **UiO-66-SO₃-3.30** measured at 30–90 °C, 85%RH, (b) Nyquist plot of **UiO-66-SO₃-3.30** measured at 30–90 °C, 93%RH, (c) Nyquist plot of **UiO-66-SO₃-3.30** measured at 30–90 °C, 98%RH.

Table S4. The optimal proton conductivity of defective UiO-66-Hf. ($\text{S}\cdot\text{cm}^{-1}$)

| modulators | the optimal proton conductivity σ ($\text{S}\cdot\text{cm}^{-1}$) | | |
|--|--|--|--|
| p-aminobenzoic acid (BA-NH ₂) | 3.82×10 ⁻² UiO-66-NH₂-3.21 | 1.53×10 ⁻² UiO-66-NH₂-3.02 | 4.56×10 ⁻² UiO-66-NH₂-3.18 |
| p-sulfobenzoic acid (BA-SO ₃) | 6.93×10 ⁻³ UiO-66-SO₃-2.36 | 3.10×10 ⁻³ UiO-66-SO₃-2.02 | 1.50×10 ⁻² UiO-66-SO₃-3.30 |

2.6. Arrhenius plots

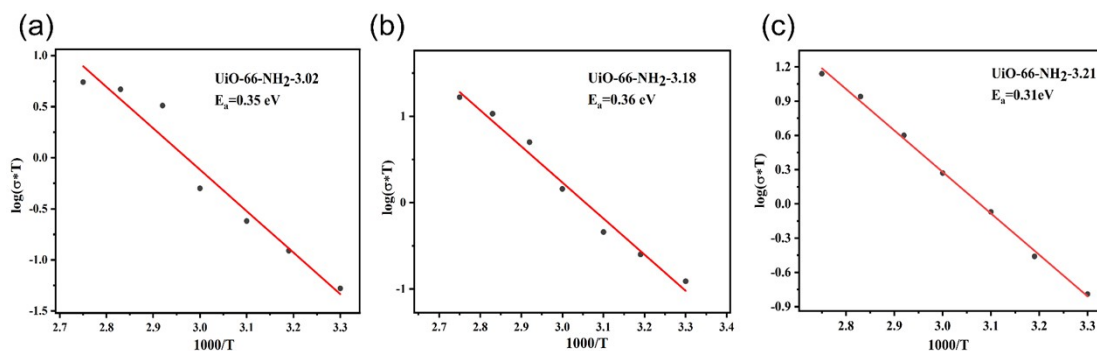


Figure S13. The Arrhenius plots of UiO-66-NH₂-x ($x = 3.02, 3.18, 3.21$) from 30 to 100 °C at 98%RH.

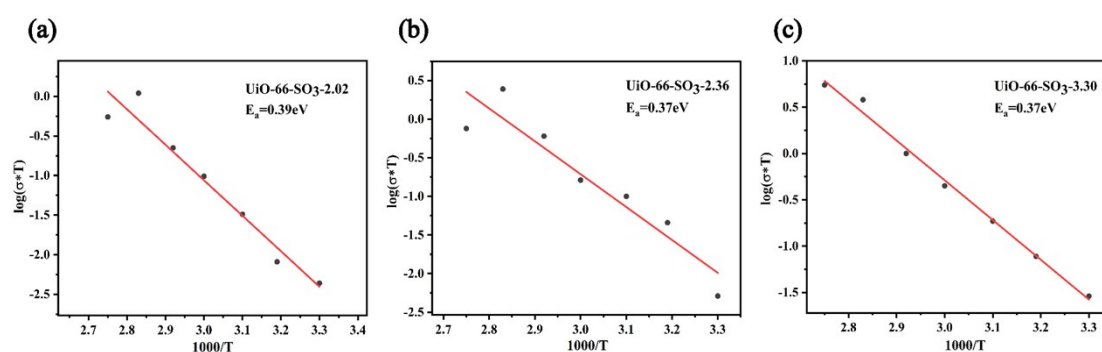


Figure S14. The Arrhenius plots of UiO-66-SO₃-x ($x = 2.02, 2.36, 3.30$) from 30 to 100 °C at 98%RH.

2.7. Water vapor adsorption

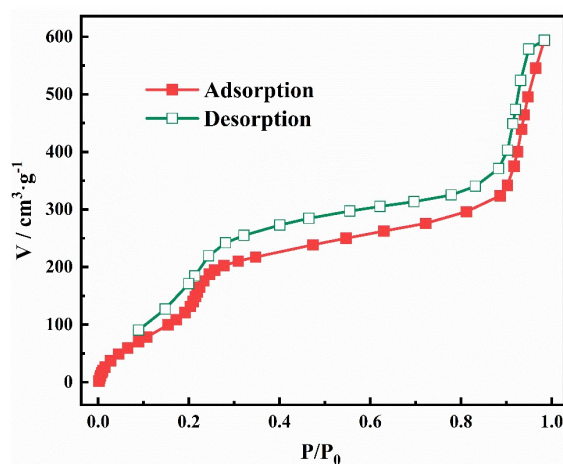


Figure S15. The water adsorption and desorption isotherm of UiO-66-NH₂-3.18. (All tests were conducted at 25°C. Filled and open symbols represent adsorption and desorption, respectively.)

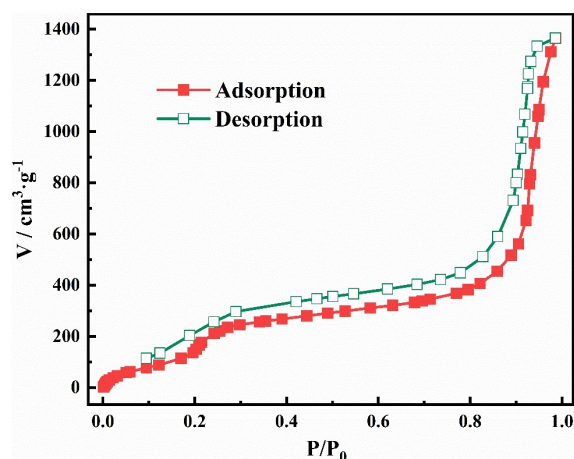


Figure S16. The water adsorption and desorption isotherm of UiO-66-SO₃-3.30. (All tests were conducted at 25°C. Filled and open symbols represent adsorption and desorption, respectively.)

2.8. Power X-Ray Diffraction (PXRD)

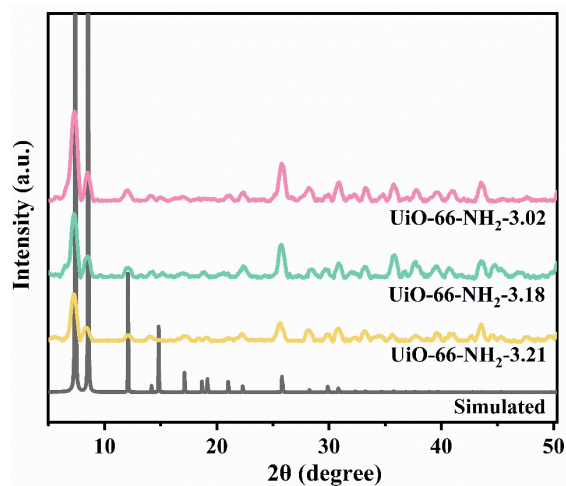


Figure S17. Powder X-ray diffraction patterns of UiO-66-NH₂-*x* (*x* = 3.02, 3.18, 3.21) and simulation. (after completing the proton conductivity measurement)

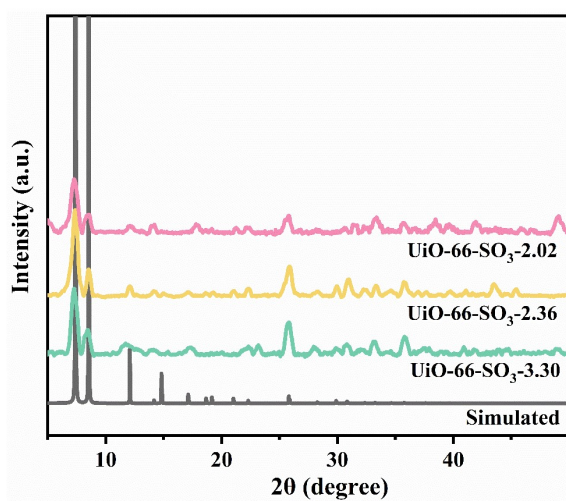


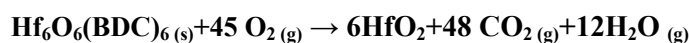
Figure S18. Powder X-ray diffraction patterns of UiO-66-SO₃-*x* (*x* = 2.02, 2.36, 3.30) and simulation. (after completing the proton conductivity measurement)

3. Quantitative Analysis Methods

The quantitative analysis part is a combination of methods reported in the previous literature, combined with thermogravimetric and nuclear magnetic to estimate the composition of the UiO-66 samples. [3]

3.1. Thermal Gravimetric Analyzer

Quantitative analysis of TGA data obtained on UiO-66-Hf is made with an important assumption: that the residue in each TGA experiment is pure HfO₂. The TGA measurements were run up to 800 °C and with a relatively slow temperature ramp (10 °C/min). Such conditions should ensure the complete combustion of organics and the conversion of hafnium to the (IV) oxide. This process can be described as:



Ideal UiO-66-Hf molecular formula: Hf₆O₄(OH)₄(BDC)₆ (molecular weight: **2186.9** g/mol)

Dehydroxylated UiO-66-Hf molecular formula: Hf₆O₆(BDC)₆ (molecular weight: **2150.9** g/mol)

UiO-66-Hf after 800 °C molecular formula: 6 HfO₂ (molecular weight: **1262.9** g/mol)

$$W_{Ideal.Plat.} = \left(\frac{M_{\text{Hf}_6\text{O}_6(\text{BDC})_6}}{M_{6\text{HfO}_2}} \right) * W_{End} \quad [4]$$

$W_{Ideal.Plat.}$ is the ideal weight of none molecular of UiO-66-Hf at 390°C.

$M_{End.}$ is the end weight of the TGA run (= **100 %** if normalized as described above).

$M_{\text{Hf}_6\text{O}_6(\text{BDC})_6}$ is the molar mass of Hf₆O₆(BDC)₆.

$M_{6\text{HfO}_2}$ is the molar mass of 6 HfO₂.

$$W_{t.PL_{Theo}} = \left(\frac{W_{Ideal.Plat.} - W_{End}}{NL_{Ideal}} \right) \quad [4]$$

NL_{Ideal} is the linkers number in the ideal Hf₆ formula unit (thus this value is 6).

W_{Ideal} is **170.3 %**.

$$x = 6 - NL_{Ideal} = 6 - \left(\frac{W_{Exp.Plat.} - W_{End}}{W_{t.PL_{Theo}}} \right) \quad [4]$$

x is the defects number of 12 samples.

$W_{Exp.Plat.}$ is the experiment weight with molecular of UiO-66-Hf at 390°C (**Figure S7–S9**).

3.2. Proton Conductivity

Weighing 30mg polycrystalline powder sample after grinding, transferring it to a steel mold with a diameter of 5 mm for tableting, and holding it at a pressure of 2 MPa for 3 minutes. Measure the thickness of each piece with a vernier caliper. The prepared sheet was connected with two Cu electrodes, and the AC impedance of the sample was tested at 30°C–90°C and 85, 93, and 98% RH, and the four-electrode method was used to test (frequency: 1 Hz-1 MHz; AC voltage amplitude: 0.01 V) is calculated by the following formula. The electrochemical impedance spectroscopy (EIS) spectra were recorded using the Nova 2 software. The proton conductivity (σ , S·cm⁻¹) was calculated using the formula :

$$\sigma = \frac{L}{RS}$$

L (cm) is the thickness of the pellet

R (Ω) is the measured impedance

S (cm²) is the flat surface area of the pellet

The activation energy was calculated from the Arrhenius equation

$$\sigma T = \sigma_0 \exp\left(\frac{-E_a}{kT}\right)$$

T (K) is the absolute temperature

E_a (eV) is the activation energy

k is the Boltzmann constant

4. References

- [1] A. Schaate, P. Roy, A. Godt, J. Lippke, F. Waltz, M. Wiebcke, P. Behrens, Modulated Synthesis of Zr-Based Metal–Organic Frameworks: From Nano to Single Crystals, *Chemistry – A European Journal*, 17 (2011) 6643-6651.
- [2] Q.-Q. Liu, S.-S. Liu, X.-F. Liu, X.-J. Xu, X.-Y. Dong, H.-J. Zhang, S.-Q. Zang, Superprotonic Conductivity of UiO-66 with Missing-Linker Defects in Aqua-Ammonia Vapor, *Inorganic Chemistry*, 61 (2022) 3406-3411.
- [3] G.C. Shearer, S. Chavan, S. Bordiga, S. Svelle, U. Olsbye, K.P. Lillerud, Defect Engineering: Tuning the Porosity and Composition of the Metal–Organic Framework UiO-66 via Modulated Synthesis, *Chemistry of Materials*, 28 (2016) 3749-3761.
- [4] S. Kim, B. Joarder, J.A. Hurd, J. Zhang, K.W. Dawson, B.S. Gelfand, N.E. Wong, G.K.H. Shimizu, Achieving Superprotonic Conduction in Metal–Organic Frameworks through Iterative Design Advances, *Journal of the American Chemical Society*, 140 (2018) 1077-1082.